Supporting Information

Regulation of the P450 oxygenation cascade involved in glycopeptide antibiotic biosynthesis

Madeleine Peschke[†, ‡], Kristina Haslinger[†,‡,¶], Clara Brieke[†], Jochen Reinstein[†], and Max J. Cryle*[,†,§]

[†]Department of Biomolecular Mechanisms, Max Planck Institute for Medical Research, Jahnstrasse 29, 69120 Heidelberg, Germany

[§]EMBL Australia, Monash University, Clayton, Victoria 3800; The Department of Biochemistry and Molecular Biology and ARC Centre of Excellence in Advanced Molecular Imaging, Monash University, Clayton, Victoria 3800

Correspondence: max.cryle@monash.edu

[‡] These authors contributed equally.

[¶] Department of Chemical Engineering, Massachusetts Institute of Technology, 77 Massachusetts Avenue, Cambridge, MA 02139

Contents

Supporting Material

NMR spectra were recorded at the University of Heidelberg/Institute for Pharmacy and Molecular Biotechnology on a Varian 500 MHz NMR spectrometer. High-resolution mass spectra were measured at the University of Heidelberg/Institute for Organic Chemistry using a Bruker Apex Qe hybrid 9.4 FT-ICR spectrometer.

1-L-CoA (H_2N-D-Hpg_1-D-Tyr_2-L-Hpg_3-D-Hpg_4-D-Hpg_5-L-Tyr_6-**L-Hpg_7**-SCoA)

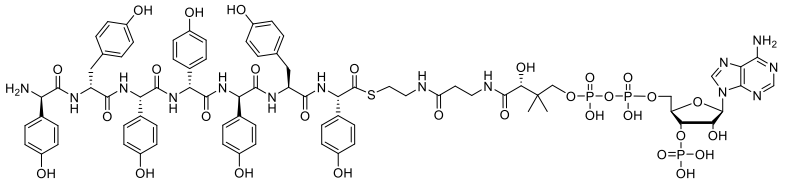

Chemical Formula: $C_{79}H_{89}N_{14}O_{30}P_3S$
Exact Mass: 1838,48
Molecular Weight: 1839,63

^{1}H-NMR (500 MHz, 1H-1H-COSY, 1H-1H-ROESY, DMSO-d_6): δ = 8.97 (d, 1H, ^3J = 6.5 Hz, Hpg_7^{NH}), 8.62 (m, 2H, Hpg_4^{NH}, Hpg_5^{NH}), 8.50 (d, 1H, ^3J = 7.8 Hz, Hpg_3^{NH}), 8.44 (d, 1H, ^3J = 7.9 Hz, Tyr_2^{NH}), 8.42 (s, 1H, H8-CoA), 8.36 (bs, 2H, NH_2-Hpg_1), 8.31 (s, 1H, ^3J = 8.0 Hz, Tyr_6^{NH}), 8.17 (s, 1H, H2-CoA), 8.09 ("t", 1H, ^3J = 5.2 Hz, N***H***CH_2CH_2S-CoA), 7.72 – 7.70 (m, 1H, N***H***CH_2CH_2CO-CoA), 7.41 (bs, 2H, NH_2), 7.24 (d, 2H, ^3J = 8.4 Hz, Hpg_1-H_{ar}-2,6), 7.20 (d, 2H, ^3J = 8.4 Hz, Hpg_7-H_{ar}-2,6), 7.01 (d, 2H, ^3J = 8.4 Hz, Hpg_4-H_{ar}-2,6), 7.24 (d, 2H, ^3J = 8.4 Hz, Hpg_1-H_{ar}-2,6), 6.99 - 6.96 (m, 4H, Hpg_3-H_{ar}-2,6, Tyr_2-H_{ar}-2,6), 6.94 (d, 2H, ^3J = 8.4 Hz, Hpg_5-H_{ar}-2,6), 6.88 (d, 2H, ^3J = 8.3 Hz, Tyr_6-H_{ar}-2,6), 6.79 – 6.76 (m, 4H, Hpg_1-H_{ar}-3,5, Hpg_7-H_{ar}-3,5), 6.61 – 6.58 (m, 8H, Tyr_2-H_{ar}-3,5, Hpg_3-H_{ar}-3,5, Hpg_4-H_{ar}-3,5, Hpg_5-H_{ar}-3,5), 6.53 (d, 2H, ^3J = 8.2 Hz, Tyr_6-H_{ar}-3,5), 5.94 (d, 1H, ^3J = 5.5 Hz, H1'-CoA), 5.52 (d, 1H, ^3J = 7.9 Hz, Hpg_3^{α}), 5.48 (d, 1H, ^3J = 7.9 Hz, Hpg_4^{α}), 5.42 (d, 1H, ^3J = 8.2 Hz, Hpg_5^{α}), 5.39 (d, 1H, ^3J = 6.4 Hz, Hpg_7^{α}), 4.85 (m, 1H, H3'-CoA), 4.79 (m, 1H, Hpg_1^{α}), 4.71 (m, 1H, H2'-CoA), 4.66 (m, 1H, Tyr_2^{α}), 4.52 (m, 1H, Tyr_6^{α}), 4.36 (m, H4'-CoA), 4.13 (m, H5'-CoA), 3.88 (m, OC$\boldsymbol{H_2^a}$C$(CH_3)_2$-CoA) 3.78 (m, C***H***(OH)CO-CoA), 3.43 (m, OC$\boldsymbol{H_2^b}$C$(CH_3)_2$-CoA), 3.34 – 3.18 (2 x m, NHC$\boldsymbol{H_2}$$CH_2$CO-CoA), 3.12 (m, 2H, NHC$\boldsymbol{H_2}$$CH_2$S-CoA), 2.96 (m, 1H, $Tyr_6^{\beta a}$), 2.92 - 2.81 (m, 2H, NHCH_2C$\boldsymbol{H_2}$S-CoA), 2.78 – 2.74 (m, 1H, $Tyr_2^{\beta a}$), 2.68 – 2.63 (m, 1H, $Tyr_2^{\beta b}$), 2.60 – 2.56 (m, 1H, $Tyr_6^{\beta b}$), 2.25 – 2.21 (m, 2H, NHCH_2C$\boldsymbol{H_2}$CO-CoA), 0.94 (s, 3H, gem-CH_3-CoA), 0.70 (s, 3H, gem-CH_3-CoA) ppm.

Numbering of Coenzyme A accords to Dordine et al. 1995.[1]

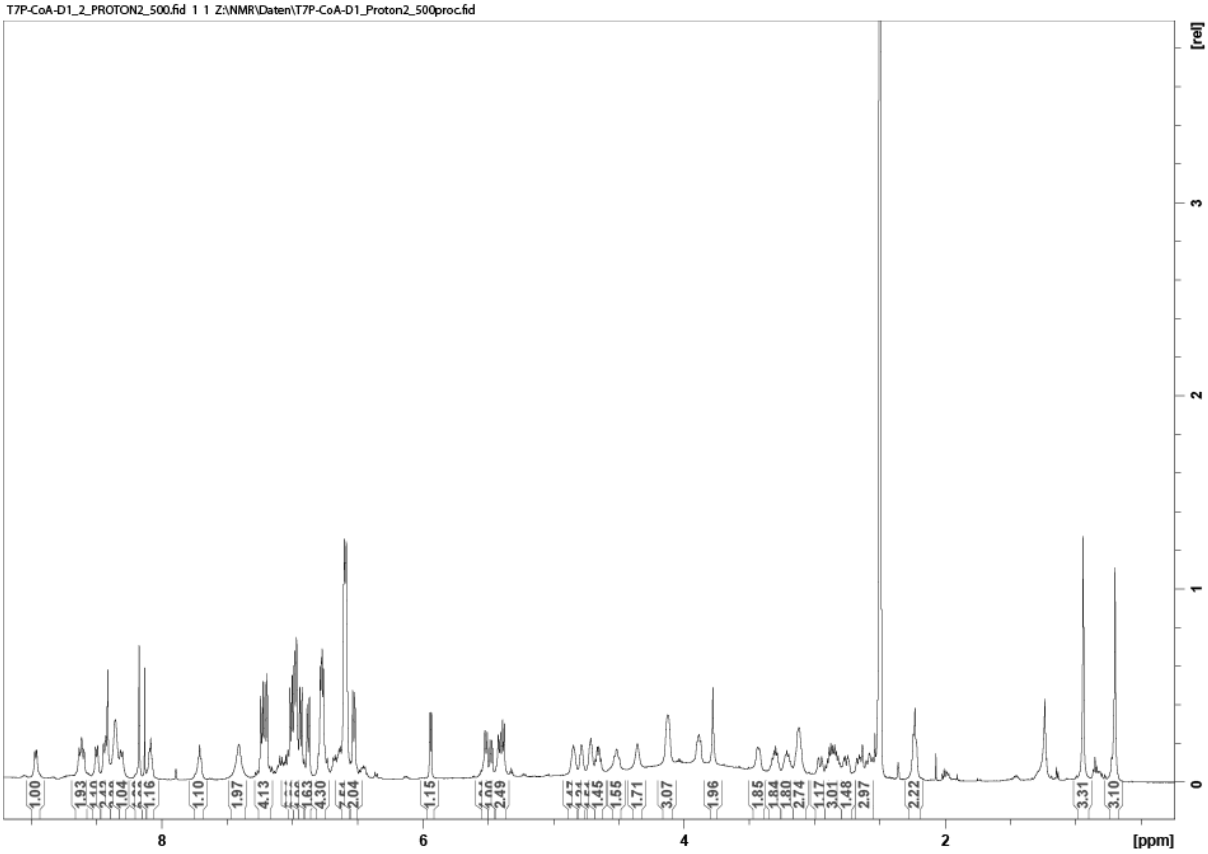

Figure S1. ^{1}H-NMR of **1-L**-CoA (500 MHz).

1-D-CoA (H_2N-D-Hpg_1-D-Tyr_2-L-Hpg_3-D-Hpg_4-D-Hpg_5-L-Tyr_6-**D-Hpg_7**-SCoA)

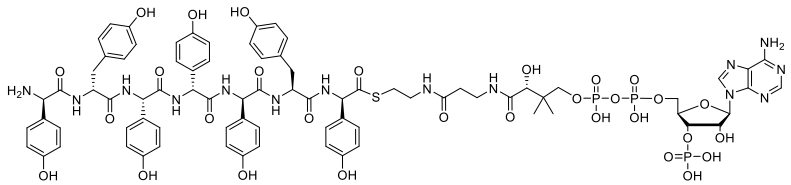

Chemical Formula: $C_{79}H_{89}N_{14}O_{30}P_3S$
Exact Mass: 1838,48
Molecular Weight: 1839,63

^{1}H-NMR (500 MHz, 1H-1H-COSY, 1H-1H-ROESY, DMSO-d_6): δ = 8.93 (d, 1H, ^{3}J = 7.1 Hz, Hpg_7^{NH}), 8.74 (d, 1H, ^{3}J = 7.7 Hz, Hpg_5^{NH}), 8.63 (d, 1H, ^{3}J = 7.9 Hz, Hpg_4^{NH}), 8.50 – 8.47 (m, 2H, Hpg_3^{NH}, Tyr_2^{NH}), 8.40 (m, 3H, H8-CoA, NH_2-Hpg_1), 8.16 (s, 1H, H2-CoA), 8.14 (m, 1H, N***H***CH_2CH_2S-CoA), 8.08 (d, 1H, ^{3}J = 7.4 Hz, Tyr_6^{NH}), 7.75 (m, 1H, N***H***CH_2CH_2CO-CoA), 7.31 (bs, 2H, NH_2), 7.24 (d, 2H, ^{3}J = 8.4 Hz, Hpg_1-H_{ar}-2,6), 7.10 (d, 2H, ^{3}J = 8.4 Hz, Hpg_7-H_{ar}-2,6), 7.07 – 7.04 (m, 4H, Hpg_4-H_{ar}-2,6, Hpg_5-H_{ar}-2,6), 7.00 – 6.97 (m, 4 H, Hpg_3-H_{ar}-2,6, Tyr_2-H_{ar}-2,6), 6.79 (d, 2H, ^{3}J = 8.4 Hz, Hpg_1-H_{ar}-3,5), 6.74 (d, 2H, ^{3}J = 8.4 Hz, Hpg_7-H_{ar}-3,5), 6.68 - 6.35 (m, 4H, $Hpg_{4/5}$-H_{ar}-3,5, Tyr_6-H_{ar}-2,6), 6.63 – 6.58 (m, 6H, Hpg_3-H_{ar}-3,5, $Hpg_{4/5}$-H_{ar}-3,5, Tyr_2-H_{ar}-3,5), 6.46 (d, 2H, ^{3}J = 8.3 Hz, Tyr_6-H_{ar}-3,5), 5.93 (d, 1H, ^{3}J = 5.5 Hz, H1'-CoA), 5.52 (d, 1H, ^{3}J = 8.1 Hz, Hpg_3^{α}), 5.51 (d, 1H, ^{3}J = 8.1 Hz, Hpg_4^{α}), 5.43 (d, 1H, ^{3}J = 7.8 Hz, Hpg_5^{α}), 5.36 (d, 1H, ^{3}J = 7.3 Hz, Hpg_7^{α}), 4.89 (m, 1H, H3'-CoA), 4.80 (m, 1H, Hpg_1^{α}), 4.70 (m, 1H, H2'-CoA), 4.65 (m, 1H, Tyr_2^{α}), 4.56 (m, 1H, Tyr_6^{α}), 4.34 (m, H4'-CoA), 4.10 (m, H5'-CoA), 3.86 (m, OC$\boldsymbol{H_2^a}$C$(CH_3)_2$-CoA) 3.80 (m, C***H***(OH)CO-CoA), 3.40 (m, OC$\boldsymbol{H_2^b}$C$(CH_3)_2$-CoA), 3.34 – 3.20 (2 x m, NHC$\boldsymbol{H_2}$$CH_2$CO-CoA), 3.17 – 3.09 (m, 2H,

NHC$\boldsymbol{H_2}$CH$_2$S-CoA), 2.89 - 2.82 (m, 2H, NHCH$_2$C$\boldsymbol{H_2}$S-CoA), 2.78 – 2.74 (m, 1H, Tyr$_2^{\beta a}$), 2.71 – 2.66 (m, 1H, Tyr$_2^{\beta b}$), 2.65 – 2.63 (m, 1H, Tyr$_6^{\beta a}$), 2.50 (under DMSO signal, Tyr$_6^{\beta b}$), 2.25 (m, 2H, NHCH$_2$C$\boldsymbol{H_2}$CO-CoA), 0.94 (s, 3H, gem-CH$_3$-CoA), 0.70 (s, 3H, gem-CH$_3$-CoA) ppm.
Numbering of Coenzyme A accords to Dordine et al. 1995.[1]

HRMS (ESI): *m*/*z* calc. for $C_{79}H_{86}N_{14}O_{30}P_3S$ $(M\text{-}3H)^{3-}$ 611.819478, found: 611.81890, Δ = 0.9 ppm; calc. mass for $C_{79}H_{87}N_{14}O_{30}P_3S$ $(M\text{-}2H)^{2-}$ 918.23285, found: 918.23495, Δ = 2.3 ppm.

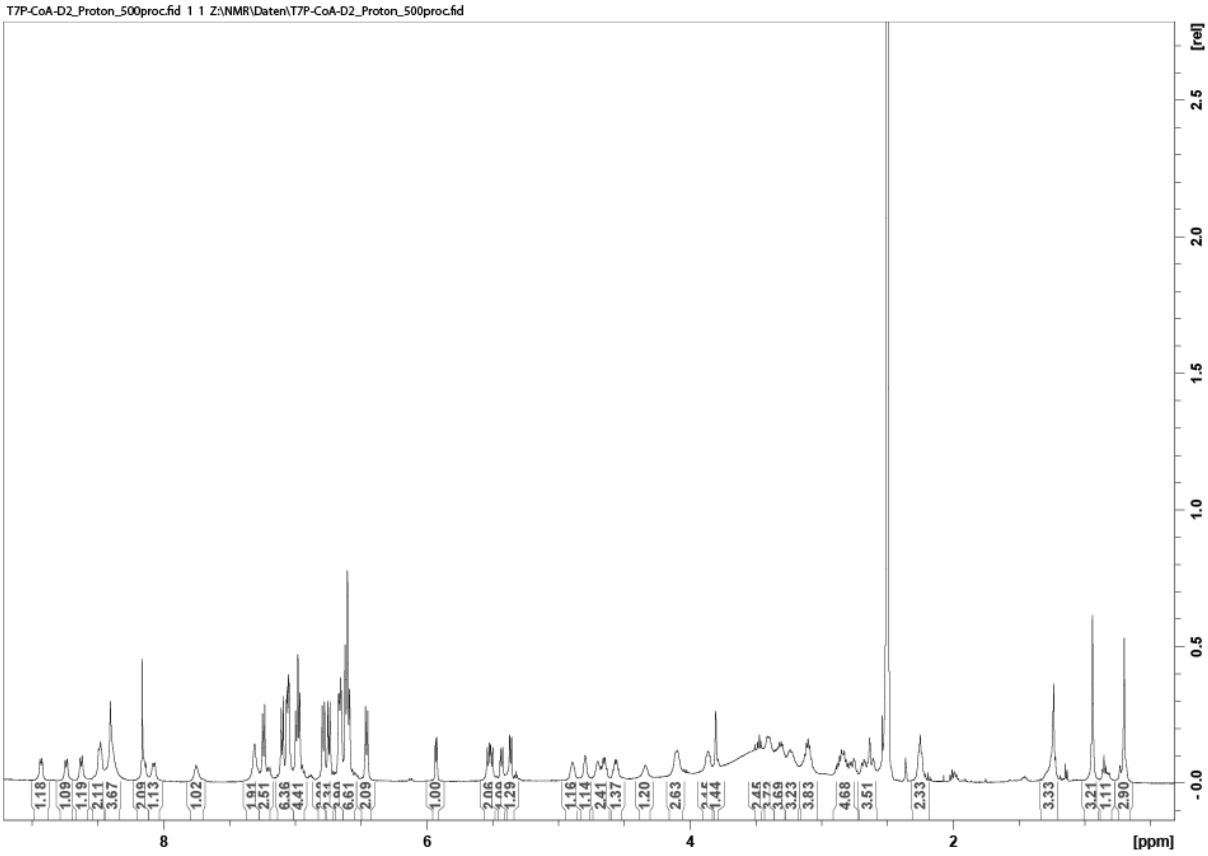

Figure S2. ^{1}H-NMR of **1-D**-CoA (500 MHz).

Supporting Methods

HPLC analysis

HPLC analysis and purifications were carried out using a High Performance Liquid Chromatograph/ Mass Spectrometer LCMS-2020 (ESI, operating both in positive and negative mode) equipped with a SPD-M20A Prominence Photo Diode Array Detector in preparative mode and a SPD-20A Prominence Photo Diode Array Detector in analytical mode, all from Shimadzu. For analytical analyses two solvent delivery LC-20AD modules were used. For preparative purifications two LC-20AP units were used.

Cloning of protein constructs

The plasmids encoding NRPS proteins used in this study comprise a natural fusion of the PCP-domain and the X-domain from module seven of the teicoplanin (Tcp12, Protein ID: Q70AZ6, PCP-X_{tei}) and vancomycin (VpsC, Protein ID: G4V4R2, PCP-X_{van}) producing NRPS machinery and have already been generated and described in other studies.[2,3] The proteins were derived from synthetic genes, codon optimized for the expression in *E. coli* obtained from Eurofins Genomics (Ebersberg, Germany). For enhanced expression and solubility the genes were cloned into a modified pET vector expressing the PCP-X di-domain proteins with IgG binding B1 domain of Streptococcus (GB1) as an N-terminal fusion partner under the control of a T7-promotor.[4] To enable a two-step affinity purification the proteins contain an N-terminal hexahistidine-tag and a C-terminal Strep-II-tag. Based on the PCP-X_{tei} construct, mutant variants (PCP-X_1, PCP-X_2, PCP-X_3, PCP-X_{1-3}) bearing amino acid substitutions in the $OxyB_{tei}$-X-domain interaction interface were generated using the In-Fusion® HD Cloning Kit (Takara Clontech, Saint-Germain-en-Laye, France). Therefore a set of internal primers bearing the mutations (amino acids numbered according to full length Tcp12 sequence): PCP-X_1 (R1211A, R1215A) fwd. CTCAGGCGCAGCTCCTGCGCGGCGTGCCCCATAG rev. CCGCGCAGGAGCTGCGCCTGAGGCTGCCCCGTTAG, PCP-X_2 (E1334A, D1335A) fwd. GTTCCAGATCGATCAGAGCTGCATCCCGCGGCAACG rev. GCCGCGGGATGCAGCTCTGATCGATCTGGAAC, PCP-X_3 (E1421A, R1426A) fwd. CAGTGCCGGCAATGCGGCCGCGTCCC rev. ATTGCCGGCACTGGCTACCAGCGTAGAGCC were used in combination with PCP and X-domain specific terminal primers. The PCP-X_{1-3} variant contains all six interface mutations and was generated in one reaction using the same primer sets. The plasmids encoding for the P450 enzymes involved in teicoplanin ($OxyB_{tei}$ (Protein ID: Q70AY8), $OxyA_{tei}$ (Protein ID: Q6ZZI8), $OxyC_{tei}$ (Protein ID: Q70AY6)) and vancomycin ($OxyB_{van}$ (Protein ID: G4V4R5)) biosynthesis were generated and described previously.[2,3,5] The P450 encoding genes from the teicoplanin biosynthetic pathway were cloned into the pET151D-TOPO (Life Technologies, Darmstadt, Germany) vector and expressed under the control of a T7 promotor with an N-terminal hexahistidine-tag followed by a V5 epitope and a Tobacco Etch Virus (TEV) protease cleavage site. The $OxyB_{van}$ encoding gene was cloned into a pET28a(+) vector and expressed under the control of a T7 promotor with an N-terminal hexahistidine-tag and a C-terminal Strep-II-tag. All generated PCP-X and P450 encoding plasmids were sequenced using standard T7 promotor and terminator primer and gene specific internal sequencing primers.

Protein expression and purification

The PCP-X proteins were expressed in the *E. coli* BL21Gold (DE3) strain (Agilent, Waldbronn, Germany) and purified by a three-step purification method including Ni-NTA- and Strep-Trap affinity chromatography followed by a final size exclusion chromatography as previously described for PCP7 proteins.[5] The expression and purification of the P450 proteins was performed as previously described

by Haslinger et al. 2014.[5] In brief, the P450s were expressed in the *E. coli* KRX strain (Promega, Mannheim, Germany) and purified by an initial Ni-NTA affinity chromatography followed by a cleavage of the N-terminal hexahistidine tag using a TEV protease (not applicable to $OxyB_{van}$). After the removal of the tag the proteins were further purified by anion exchange (ResourceQ, GE Healthcare, Munich) and size exclusion chromatography (Superose12 10/300 GL, GE Healthcare, Munich).

Loading of *peptidyl*-CoA onto *apo*-PCP-X proteins

Prior UV-visible spectroscopy and *in vitro* P450 turnover reactions the heptapeptide-CoA conjugates were loaded to the respective *apo*-PCP-X proteins from the teicoplanin and vancomycin system. The loading reaction was performed by using the phosphopantetheinyl transferase Sfp variant R4-4[6] for 1h at 30°C (60 µM PCP-X, 120 µM *peptidyl*-CoA, 6 µM Sfp, 50 mM Hepes pH 7.0, 50 mM NaCl, 10 mM $MgCl_2$). Following the reaction the excess of unbound peptide was removed by a dilution-concentration procedure using centrifugal filter units with a 10,000 MW cut-off (Merck Millipore, Darmstadt, Germany) and low salt buffer (50 mM Hepes pH 7.0, 50 mM NaCl for turnovers and 20 mM Hepes pH 7.0, 50 mM NaCl for UV-visible spectroscopy 4x 1:5 dilution). The *peptidyl*-PCP-X proteins were directly used for UV-visible spectroscopic measurements and P450 *in vitro* activity assays.

Modified $OxyB_{tei}$-catalyzed turnover for UV-visible studies

To analyze the binding of monocyclic substrate peptides to the P450s, *peptidyl*-PCP-X was subjected to initial $OxyB_{tei}$-mediated cyclization. In order to minimize the influence of the turnover components on the UV-visible spectrum the concentration of $OxyB_{tei}$ was reduced 16-fold compared to standard turnover conditions: no decrease in the production of monocyclic peptide was observed.[3] The concentration of the components of the redox system was reduced according to the reduced $OxyB_{tei}$ concentration (final reaction mix: 200:1:5:1 ratio (PCP:PuR:PuxB:OxyB), 0.3 mM NADH (no NADH regeneration); 2h, 30°C). After the incubation, NADH was removed by repeated washing using low salt buffer 20 mM Hepes pH 7.0, 50 mM NaCl (4x 1:5 dilution) in centrifugal filter units with a 10,000 MW cut-off (Merck Millipore, Darmstadt, Germany). The monocyclic *peptidyl*-PCP-X was concentrated to 200-600 µM and immediately used for titrations. After the titration experiments the turnover yield was determined by HPLC-MS analysis. The concentrations of all *peptidyl*-PCP-X samples were determined by the method of Ehresmann et al.[7] and the complete removal of NADH in the $OxyA_{tei}$ probes was confirmed by measuring the absorption at $\lambda = 340$ nm.

Global fit analysis of UV-visible spectroscopic data

UV-visible spectroscopic data obtained from titrations of $OxyB_{tei}$ and $OxyA_{tei}$ with various *peptidyl*-PCP-X conjugates were subjected to global fit analysis by DynaFit4[8] together with a non-linear uncertainty assessment by a Monte-Carlo algorithm (1,000 iterations) in four sets: $OxyB_{tei}$ titrated with three linear peptide conjugates, $OxyB_{tei}$ titrated with three monocyclic peptide conjugates, $OxyA_{tei}$ titrated with three linear peptide conjugates and $OxyA_{tei}$ titrated with three monocyclic peptide conjugates. The underlying reaction mechanism and parameters are given in the commented input script below for one such set (not all input files are listed):

```
[task]              ; section defining the tasks for DynaFit4

   data = equilibria
   task = fit        ; as opposed to simulate
   confidence = monte-carlo   ; non-linear uncertainty assessment method, 1,000 iterations
   model = one_step_binding; one step binding of three different peptidyl-PCPX conjugates to
                           P450s (from now on called LpPX, DpPX and L_DpPX

[mechanism]           ; section defining the reaction mechanism in direction of dissociation

   OxyLpPX  <===> Oxy + LpPX : KdLpPX equil ; first step
   OxyDpPX  <===> Oxy + DpPX : KdDpPX equil ; first step
   OxyL_DpPX  <===> Oxy + L_DpPX : KdL_DpPX equil ; first step


[parameters]          ; section defining the global parameters (P450 concentrations, here
                      given as constant)

   cOxy1 = 2.0 ; micromolar
   cOxy2 = 2.6 ; micromolar

[constants]           ; initial values for the dissociation constants (to be fitted)
   KdLpPX= 1.3 ?;
   KdDpPX = 1.3 ?;
   KdL_DpPX = 1.3 ?;

[responses]           ; initial values for the P450 response normalized by concentration
                      (parameters marked with "?" will be fitted)

   OxyLpPX = 0.08 ?
   OxyDpPX = 0.08 ?
   OxyL_DpPX = 0.08 ?

[output]
   directory current\output
[data]
   directory      current\data
   extension      txt

        variable       LpPX          ; data files with LpPX varied at 2 P450 concentrations
                                    (if applicable)

                file LpPX_1 | conc  Oxy = 1 * cOxy1         ; data with 1st P450 concentration
                file LpPX_4 | conc  Oxy = 1 * cOxy2         ; data with 2nd P450 concentration

        variable       DpPX          ; data files with DpPX varied

                file DpPX_1 | conc  Oxy = 1 * cOxy2

        variable       L_DpPX        ; data files with L_DpPX varied

                file L_DpPX_1 | conc  Oxy = 1 * cOxy2
====-> more input data files
[end]
```

UV-visible spectroscopic data for the competition of the X-domain or the PCP-X didomain (*apo*/*holo*) with the *peptidyl*-PCP-X didomain for $OxyB_{tei}$ were subjected to global fit analysis by DynaFit4[8] together with a non-linear uncertainty assessment by a Monte-Carlo algorithm (1,000 iterations). The underlying reaction mechanism and parameters are given in the commented input script below (not all input files are listed):

```
[task]              ; section defining the tasks for DynaFit4

   data = equilibria
   task = fit        ; as opposed to simulate
   confidence = monte-carlo   ; non-linear uncertainty assessment method, 1,000 iterations
   model = one_step_competition; one step competition of X-domain/apo-/holo-PCPX di-domain
                               (from now on called X, aPX and hPX) and peptidylPCPX (from
                               now on called pPX)

[mechanism]           ; section defining the reaction mechanism

   OxypPX  <===> Oxy + pPX : KdpPX equil ; first step
   OxyX  <===> Oxy + X : KdX equil ; first step
   OxyaPX  <===> Oxy + aPX : KdaPX equil ; first step
   OxyhPX  <===> Oxy + hPX : KdhPX equil ; first step

[parameters]          ; section defining the global parameters (P450 concentrations,
                      constant)

   cOxy1 = 2.0 ; micromolar
   cOxy2 = 2.6 ; micromolar

[constants]           ; initial values for the dissociation constants (to be fitted)

   KdpPX = 1.3 ?
   KdX = 1 ? ;
   KdaPX = 10 ?;
   KdhPX = 10 ?;

[responses]           ; initial values for the P450 response normalized by concentration
                      (parameters marked with "?" will be fitted)

   OxypPX = 0.08 ?
   OxyX = 0.00
   OxyaPX = 0.00
   OxyhPX = 0.00

[output]
   directory current\output
[data]
   directory      current\data
   extension      txt

       variable       pPX          ; data files with pPX varied at 2 P450 concentrations (if
                                   applicable)
              file pPX_1 | conc  Oxy =   1 * cOxy1        ; data with 1st P450 concentration
              file pPX_4 | conc  Oxy =   1 * cOxy2        ; data with 2nd P450 concentration

       variable       X            ; data files with X varied at 3 concentrations of pPX

              file X_2_5 | conc Oxy = 1 * cOxy1, pPX = 2.5 ; concentrations pPX in micromolar
              file X_5   | conc Oxy = 1 * cOxy1, pPX = 5
              file X_10  | conc Oxy = 1 * cOxy1, pPX = 10

       variable       aPX          ; data files with aPX varied at 3 concentrations of pPX

              file aPX_5 | conc Oxy = 1 * cOxy2, pPX = 5

       variable       hPX          ; data files with aPX varied at 3 concentrations of pPX

              file hPX_5 | conc Oxy = 1 * cOxy2, pPX = 5

====-> more input data files
 [end]
```

CD spectroscopy of the PCP-X_{tei} wild type and mutant proteins

CD-spectroscopy was performed in 50 mM sodium phosphate buffer pH 7.4 at a protein concentration of 5 µM in a glass cuvette (path length of 0.1 cm, Hellma). The measurements were performed at 20°C with a Jasco J-810 CD-Spectropolarimeter (Jasco) by recording the wavelength dependent ellipticity at λ = 200 to 260 nm. Melting curves were recorded at λ = 222 nm in a temperature range from 20 to 95°C by applying a ramp of 1°C/min. The mean residue ellipticity $[\theta]_{mrw,\lambda}$ was calculated in order to compare the generated spectra. The melting temperatures were analyzed by performing a Boltzmann sigmoidal non-linear fit.

Supporting Results

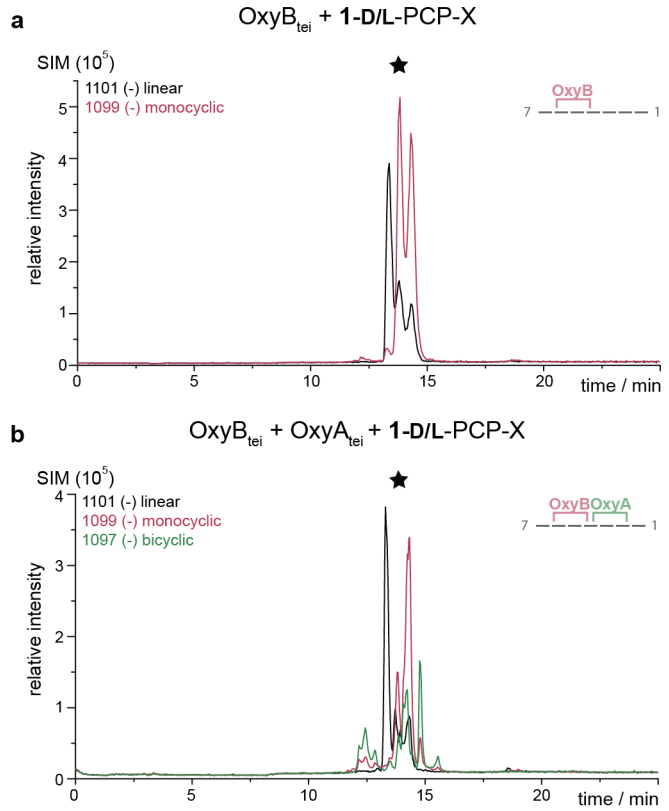

Figure S3. HPLC-MS analysis of OxyB$_{tei}$-catalyzed cyclization of **1-D/L**-PCP-X$_{tei}$ (**a**) compared to OxyB$_{tei}$/OxyA$_{tei}$ coupled turnover (**b**) using single ion monitoring. Black: *m/z* signal detected over time corresponding to the linear peptide; red: *m/z* corresponding to the monocyclic peptide; green: *m/z* corresponding to the bicyclic peptide; asterisk highlights one of the two dominant peaks belonging to the diastereomers of the monocyclic peptide (due to racemization of Hpg$_7$) – the area of this peak decreases in the coupled turnover compared to the OxyB$_{tei}$ turnover, while the other one remains practically unchanged.

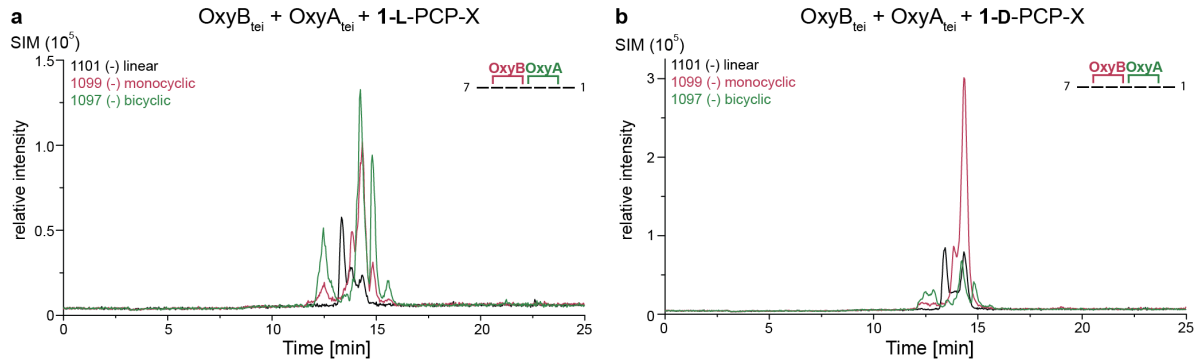

Figure S4. HPLC-MS analysis of $OxyB_{tei}$/$OxyA_{tei}$ coupled turnover with the separated diastereomers of peptide **1** loaded onto PCP-X as substrates using single ion monitoring. **1-L**-PCP-X_{tei} (**a**), **1-D**-PCP-X_{tei} (**b**); Black: *m/z* signal detected over time corresponding to the linear peptide; red: *m/z* corresponding to the monocyclic peptide; green: *m/z* corresponding to the bicyclic peptide.

Table S1. Summary of data obtained for the coupled $OxyB_{tei}$/$OxyA_{tei}$ *in vitro* activity assay in comparison to the literature values for $OxyB_{tei}$ and coupled $OxyB_{tei}$/$OxyA_{tei}$ turnover[2,3]. Reference values for monocyclic and bicyclic product formation – originally expressed as the percentage of total peptide detected – were transformed to $OxyB_{tei}$ and $OxyA_{tei}$ activities for comparison (percentage of substrate converted). Results obtained from triplicate experiments including the standard deviation.

P450s		*peptide*	*PCP-X*	*C-O-D ring formation [%]*	*D-O-E ring formation [%]*	*reference*
$OxyB_{tei}$	-	***1-D/L***	*PCP-X*	*67 ± 3*	-	*Haslinger et al. 2015*[2]
$OxyB_{tei}$	-	***1-D/L***	*PCP-X*	*66 ± 1*	-	*Brieke et al. 2015*[3]
$OxyB_{tei}$	*$OxyA_{tei}$*	***1-D/L***	*PCP-X*	*78 ± 1*	*48 ± 6*	*Haslinger et al. 2015*[2]
$OxyB_{tei}$	*$OxyA_{tei}$*	***1-D/L***	*PCP-X*	*67 ± 5*	*36 ± 2*	*Brieke et al. 2015*[3]
$OxyB_{tei}$	-	***1-D/L***	*PCP-X_2*	*64 ± 4*	-	*Haslinger et al. 2015*[2]
$OxyB_{tei}$	*$OxyA_{tei}$*	***1-D/L***	*PCP-X_2*	*62 ± 1*	*24 ± 2*	*This work*
$OxyB_{tei}$	-	***1-D/L***	*PCP-X_3*	*70 ± 1*	-	*Haslinger et al. 2015*[2]
$OxyB_{tei}$	*$OxyA_{tei}$*	***1-D/L***	*PCP-X_3*	*67 ± 1*	*34 ± 3*	*This work*
$OxyB_{tei}$	*$OxyA_{tei}$*	***1-L***	*PCP-X*	*91 ± 1*	*64 ± 2*	*This work*
$OxyB_{tei}$	*$OxyA_{tei}$*	***1-D***	*PCP-X*	*88 ± 1*	*26 ± 1*	*This work*

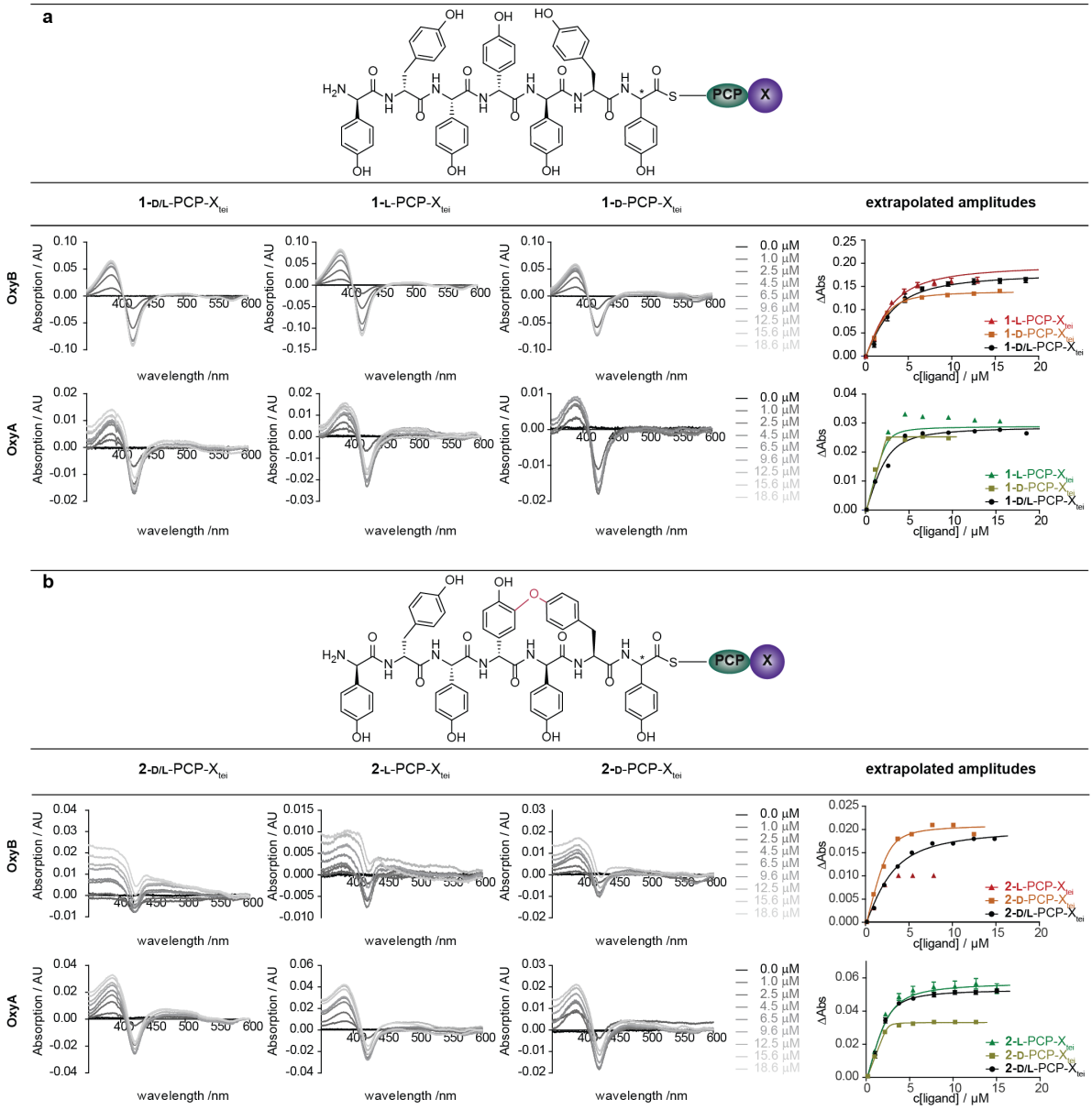

Figure S5. UV-visible spectroscopic binding studies of *peptidyl*-PCP-X_{tei} binding to $OxyB_{tei}$ and $OxyA_{tei}$; Linear peptides (**a**), monocyclic peptides (**b**).

Table S2. UV-visible binding studies of **1**- and **2**-PCP-X_{tei} conjugates to $OxyB_{tei}$ and $OxyA_{tei}$.

1-PCP-X binding to $OxyB_{tei}$					
Parameter	*Value*	*SE*	*Mean*	*Min*	*Max*
K_D (**1-L**-PCP-X_{tei}) [μM]	1.26	0.14	1.27	0.78	1.73
ΔA_{max} (**1-L**-PCP-X_{tei})	0.077	1.7E-03	0.077	0.071	0.083
K_D (**1-D**-PCP-X_{tei}) [μM]	0.43	0.20	0.45	0.04	1.44
ΔA_{max} (**1-D**-PCP-X_{tei})	0.055	2.5E-03	0.055	0.047	0.065
K_D (**1-D/L**-PCP-X_{tei}) [μM]	1.39	0.204	1.41	0.86	2.25
ΔA_{max} (**1-D/L**-PCP-X_{tei})	0.070	1.8E-03	0.070	0.065	0.076
2-PCP-X binding to $OxyB_{tei}$					
Parameter	*Value*	*SE*	*Mean*	*Min*	*Max*
K_D (**2-L**-PCP-X_{tei}) [μM]	n.d.[a]	n.d.	n.d.	n.d.	n.d.
ΔA_{max} (**2-L**-PCP-X_{tei})	0.004	2.2E-04	0.004	0.004	0.005
K_D (**2-D**-PCP-X_{tei}) [μM]	0.30	0.09	0.31	0.08	0.62
ΔA_{max} (**2-D**-PCP-X_{tei})	0.008	2.2E-04	0.008	0.008	0.009
K_D (**2-D/L**-PCP-X_{tei}) [μM]	1.49	0.29	1.50	0.92	2.60
ΔA_{max} (**2-D/L**-PCP-X_{tei})	0.008	3.2E-04	0.008	0.007	0.009
1-PCP-X binding to $OxyA_{tei}$					
Parameter	*Value*	*SE*	*Mean*	*Min*	*Max*
K_D (**1-L**-PCP-X_{tei}) [μM]	0.14	0.090	0.15	0.00	0.62
ΔA_{max} (**1-L**-PCP-X_{tei})	0.013	4.4E-04	0.013	0.012	0.014
K_D (**1-D**-PCP-X_{tei}) [μM]	n.d.[a]	n.d.	n.d.	n.d.	n.d.
ΔA_{max} (**1-D**-PCP-X_{tei})	0.011	6.2E-04	0.011	0.010	0.014
K_D (**1-D/L**-PCP-X_{tei}) [μM]	0.59	0.230	0.60	0.15	1.73
ΔA_{max} (**1-D/L**-PCP-X_{tei})	0.013	5.4E-04	0.013	0.011	0.014
2-PCP-X binding to $OxyA_{tei}$					
Parameter	*Value*	*SE*	*Mean*	*Min*	*Max*
K_D (**2-L**-PCP-X_{tei}) [μM]	0.54	0.12	0.54	0.18	1.02
ΔA_{max} (**2-L**-PCP-X_{tei})	0.025	7.1E-04	0.025	0.023	0.028
K_D (**2-D**-PCP-X_{tei}) [μM]	n.d.[a]	n.d.	n.d.	n.d.	n.d.
ΔA_{max} (**2-D**-PCP-X)	0.014	9.0E-04	0.014	0.012	0.019
K_D (**2-D/L**-PCP-X_{tei}) [μM]	0.36	0.116	0.37	0.10	0.83
ΔA_{max} (**2-D/L**-PCP-X_{tei})	0.023	6.8E-04	0.023	0.021	0.025

Global data analysis based on a simple 1:1 binding mechanism for different peptides. Values for KD and maximal signal amplitudes (ΔA_{max}, normalized by the P450 concentration) were fitted with the program Dynafit[8] (script 1) with corresponding Standard Error (SE). A robust non-linear uncertainty assessment was obtained from Monte-Carlo analysis (Min, Max define uncertainty interval, 1000 iterations). [a] active site titration with the saturation reached at ~2 μM (a 1:1 complex); the information derived from the collected data points does not allow an accurate extrapolation of the K_D.

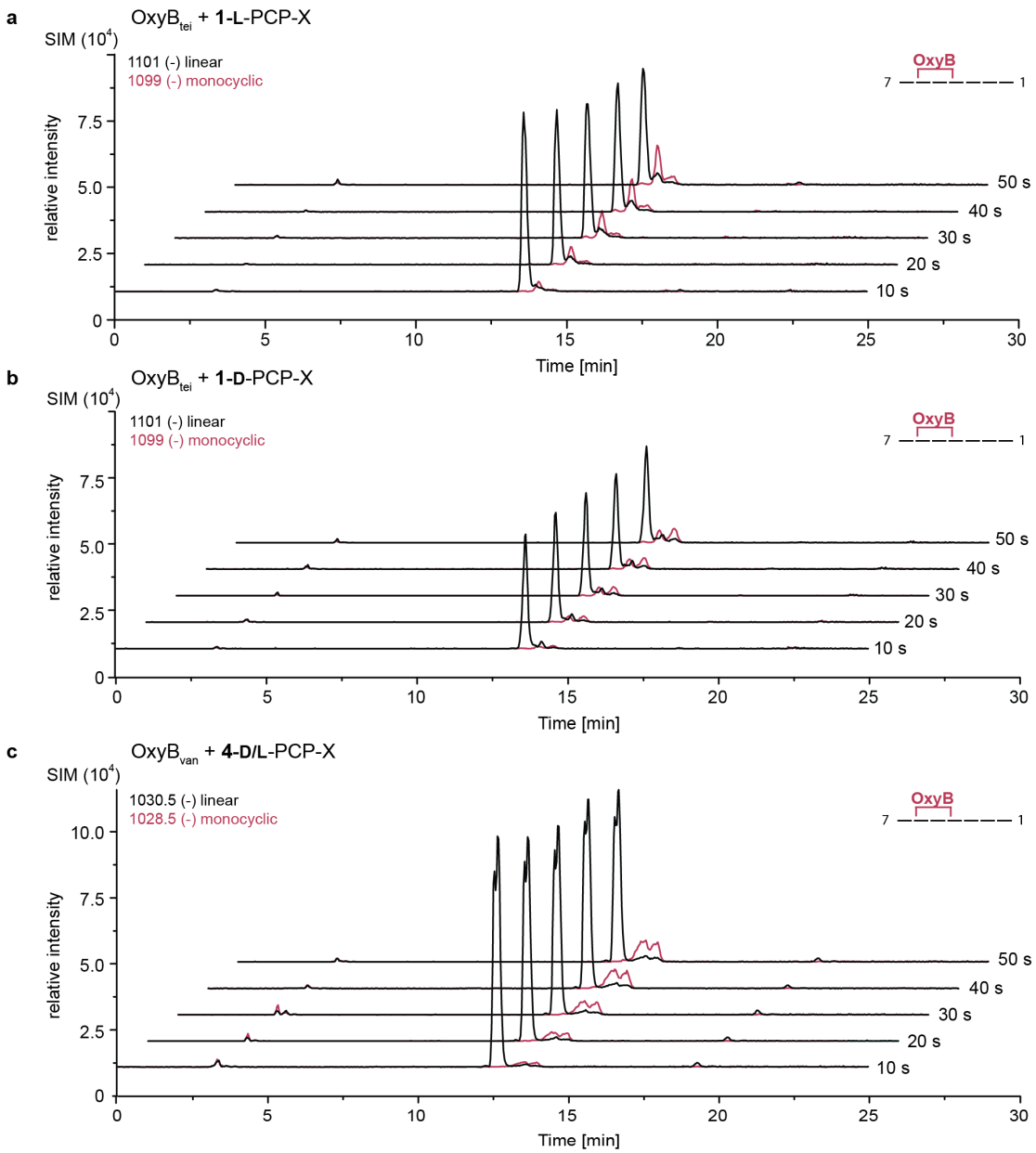

Figure S6. HPLC-MS traces of various time points of OxyB-catalyzed turnover of *peptidyl*-PCP-X. OxyB$_{tei}$: 1.25 µM **1-L**-PCP-X$_{tei}$ (**a**), 1.25 µM **1-D**-PCP-X$_{tei}$ (**b**) and OxyB$_{van}$: 15 µM **4-D/L**-PCP-X$_{van}$ (**c**); Black: *m/z* signal detected over time corresponding to the linear peptide; red: *m/z* corresponding to the monocyclic peptide.

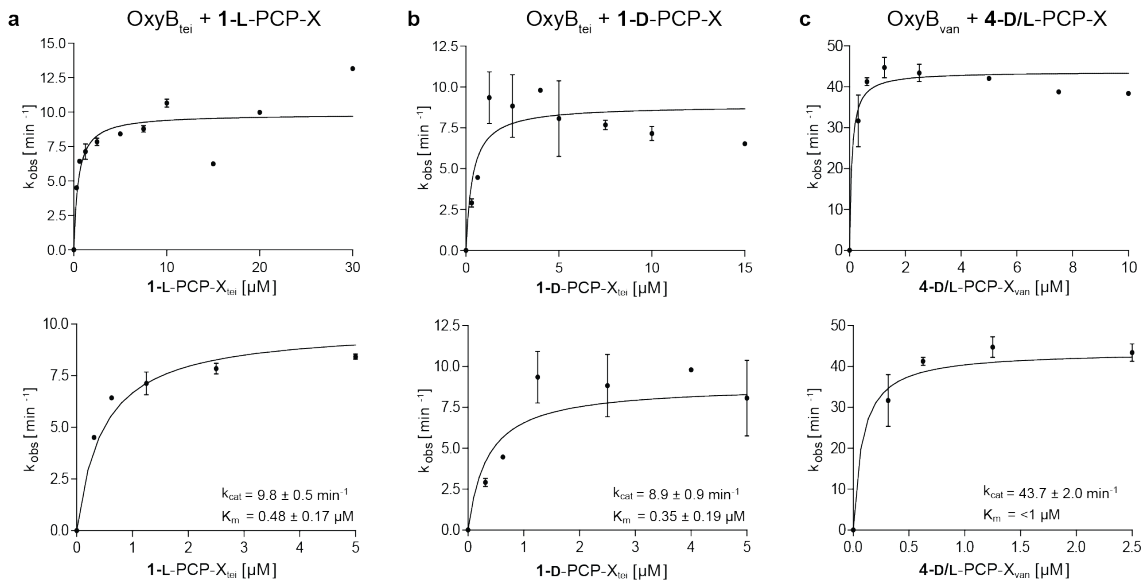

Figure S7. Overview of the kinetic parameters determined for OxyB$_{tei}$ with **1-L**-PCP-X$_{tei}$ (**a**) and **1-D**-PCP-X$_{tei}$ (**b**) as a substrate and OxyB$_{van}$ with **4-D/L**-PCP-X$_{van}$ as the substrate (**c**). Full representation of the data points obtained from steady state kinetics (upper panel), zoomed version closer into the data section for lower substrate concentrations (lower panel).

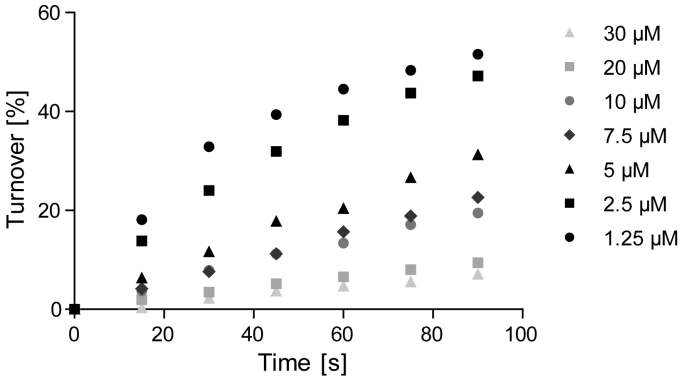

Figure S8. Representative plot of turnover yields over time used to extrapolate initial velocities for OxyB$_{tei}$–catalyzed (0.125 μM) turnover at various substrate concentrations (**1-L**-PCP-X$_{tei}$). The initial linear range of the progression curve was used to calculate the kinetic parameters shown in Figure S7.

Supplementary note regarding $OxyB_{tei}$ kinetics:

The progression curves from the kinetic measurements (example see SI Figure S8) can be used to roughly estimate the K_Dp (dissociation constant of the product) using the following equation:

$$v = V_{max} \frac{S}{S + K_M(1 + \frac{P}{K_D p})}$$

v = v(t) observed velocity at specific time point
V_{max} = initial velocity of the progression curve
S = [S(t)] substrate concentration at specific time point
P = [P(t)] product concentration at specific time point
K_M = K_M obtained from the steady state kinetics
K_Dp = dissociation constant of the product

Supplementary note regarding $OxyB_{van}$ kinetics:

For $OxyB_{van}$ we determined a k_{cat} of 43.7 ± 2.0 min^{-1} (SI Figure S8C, Table S2), which is 6.5 times higher than the k_{cat} reported for the vancomycin hexapeptide coupled to the PCP-domain from module seven as a substrate.[9] At the same time, the K_M for the vancomycin-type heptapeptide is <0.1 µM, at least 130 times lower than the reported K_M for the hexapeptide. This is in good agreement with our binding studies, which show a more than 10-fold increase in binding affinity in presence of the X-domain (K_D <1 µM compared to 17 µM reported by Woithe et al. 2007) (SI Figure S14). In comparison to the data obtained with $OxyB_{tei}$ for the teicoplanin-like heptapeptide, the K_M for $OxyB_{van}$ is at least 4 times smaller, whilst the k_{cat} is more than 4 times higher.

Table S3. Summary of kinetic parameters determined for $OxyB_{tei}$ and $OxyB_{van}$.

P450s	*peptide*	*PCP-X*	*k_{cat} [min^{-1}]*	*+/- SE*	*K_M [µM]*	*+/- SE*
$OxyB_{tei}$	***1-L***	*$PCP\text{-}X_{tei}$*	*9.8*	*0.5*	*0.48*	*0.17*
$OxyB_{tei}$	***1-D***	*$PCP\text{-}X_{tei}$*	*8.9*	*0.9*	*0.35*	*0.19*
$OxyB_{van}$	***4-D/L***	*$PCP\text{-}X_{van}$*	*43.7*	*2.0*	*< 0.1**	*n.d.*

* sensitivity of the assay does not allow the exact determination of this value

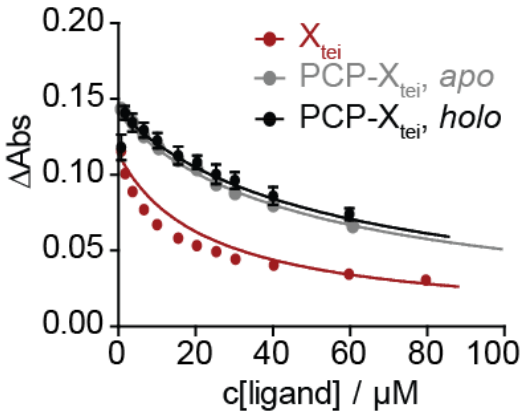

Figure S9. Extrapolated amplitudes of the spectral response upon **1-L**-PCP-X displacement from $OxyB_{tei}$ by titration with the isolated X-domain (red), *apo*-(grey) or *holo*-PCP-X di-domain (black).

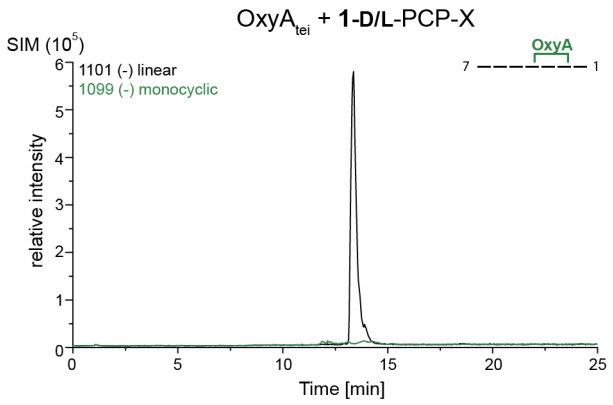

Figure S10. HPLC-MS analysis of OxyA$_{tei}$-catalyzed turnover of linear **1-D/L** peptide coupled to PCP-X$_{tei}$. Black: *m/z* signal detected over time corresponding to the linear peptide; green: *m/z* corresponding to the monocyclic peptide.

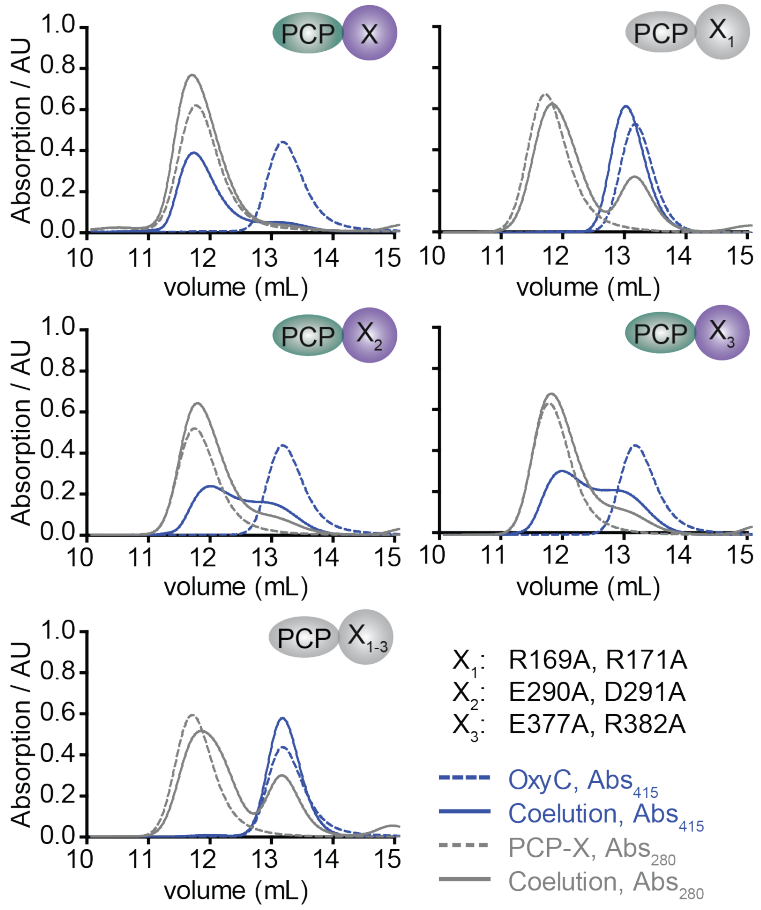

Figure S11. Analytical size exclusion chromatography of $OxyC_{tei}$ with PCP-X_{tei} wild type and mutant variants of the PCP-X didomain. Dashed lines: elution profile of the individual proteins, solid lines: co-elution profile of a 3:1 mixture of the PCP-X di-domain and the respective P450, with detection either at λ = 280 nm (grey) or 415 nm (heme absorption, blue).

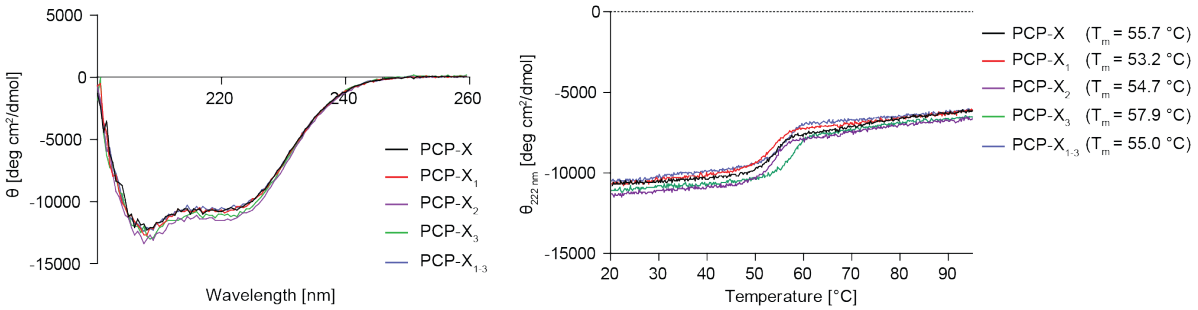

Figure S12. Circular dichroism (CD) spectra and melting curve analysis of the GB1-PCP-X wild type protein and the mutant variants.

To confirm the native folding of the PCP-X domains variants carrying mutations in the main regions involved in the $OxyB_{tei}$ binding, CD spectroscopy was performed. The recorded far-UV CD spectra for all proteins demonstrate the existence of two distinct minima at $\lambda = 208$ and $\lambda = 222$ nm, which is comparable to the wild type PCP-X protein. Furthermore, the thermal stability of the protein variants was analyzed through the loss of the helical content at 222 nm upon heating. No complete unfolding of the proteins was observed, likely caused by the N-terminal GB1-fusion partner that has been shown to possess high thermal stability.[10] In spite of the stability of the proteins, a well-defined transition was observed for all the proteins: this showed a thermal transition midpoint (T_m) in the range from 53 to 58°C for the different proteins. These results confirm the structural integrity of the mutant variants and thus show that the absence of binding to the P450s in the case of PCP-X_1 and PCP-X_{1-3} is not a result of the misfolding of the mutant variants.

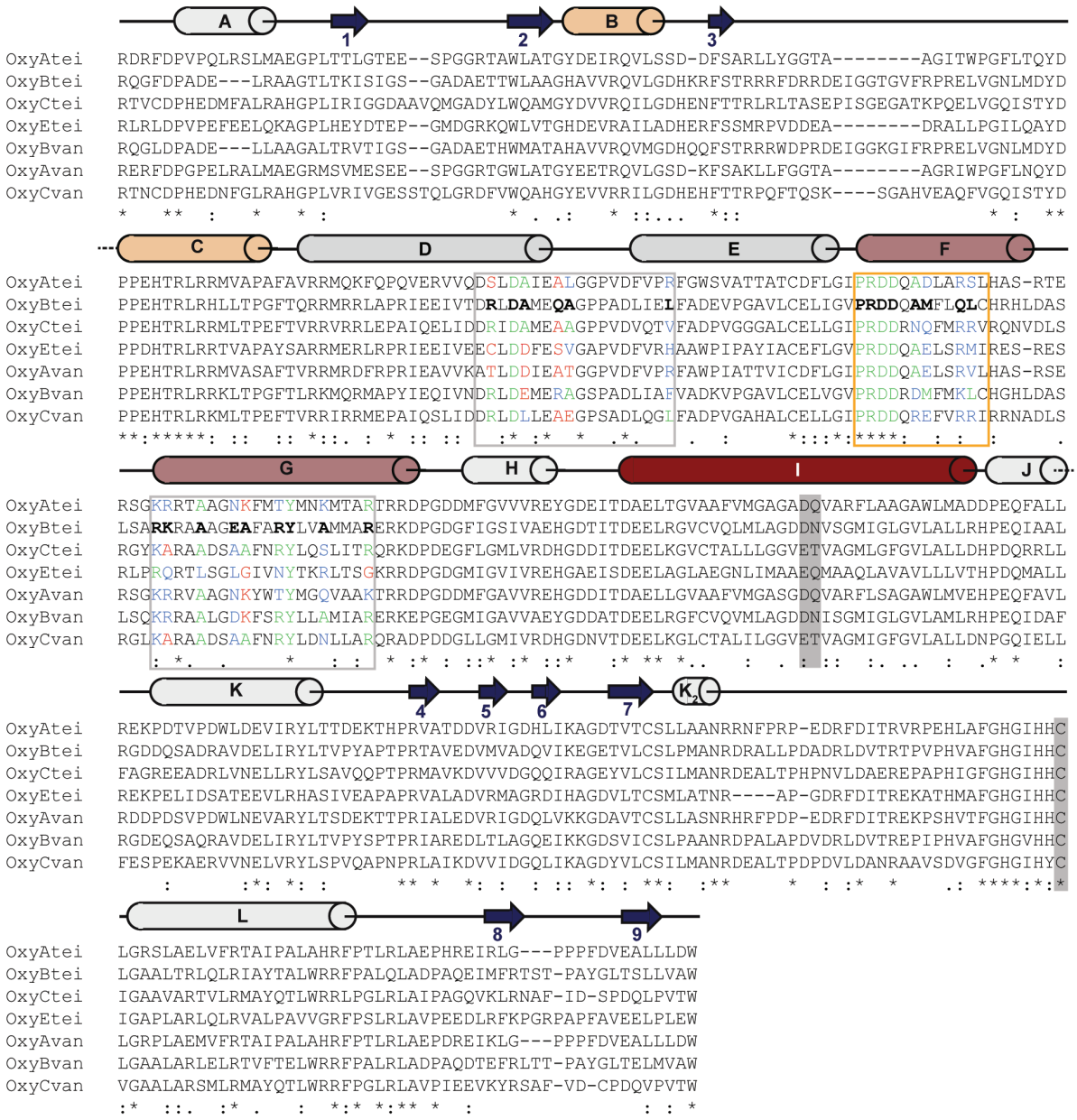

Figure S13. Alignment of the peptide-tailoring Oxy enzymes involved in teicoplanin biosynthesis ($OxyA_{tei}$, $OxyB_{tei}$, $OxyC_{tei}$ and $OxyE_{tei}$) and vancomycin biosynthesis ($OxyA_{van}$, $OxyB_{van}$, $OxyC_{van}$) with the secondary structure of $OxyB_{tei}$ displayed as cartoon and labeled according to the canonical secondary structure elements of P450 enzymes. Grey shaded residues: catalytically important P450 amino acid residues – I-helix acid/ (alcohol/ amide) pair and heme coordinating cysteine residue; grey boxes: regions experimentally shown to interact with the X-domain (not essential for recruitment and catalysis); orange box: region experimentally shown to interact with the X-domain (essential for recruitment and catalysis) including the highly conserved PRDD motif; emboldened residues are involved in direct interactions with the X-domain; green/blue/red colored residues indicate identical/similar/dissimilar residues in other Oxy proteins.

Table S4. Summary of data obtained for the $OxyB_{tei}$ *in vitro* activity assay in presence or absence of competing Oxy enzymes ($OxyA_{tei}$ or $OxyC_{tei}$) after 5 s reaction time. In reactions containing a second P450 no additional second ring closure was observed. Results obtained from triplicate experiments including the standard deviation.

Timing	*2nd P450*	*peptidyl-PCP-X substrate*	*C-O-D ring formation [%]*
OxyB first	-	***1-L**-PCP-X_{tei}*	*56 ± 7*
	$OxyA_{tei}$	***1-L**-PCP-X_{tei}*	*30 ± 3*
	$OxyC_{tei}$	***1-L**-PCP-X_{tei}*	*38 ± 4*
Same time	-	***1-L**-PCP-X_{tei}*	*51 ± 4*
	$OxyA_{tei}$	***1-L**-PCP-X_{tei}*	*20 ± 2*
	$OxyC_{tei}$	***1-L**-PCP-X_{tei}*	*22 ± 2*
OxyB second	*$OxyA_{tei}$*	***1-L**-PCP-X_{tei}*	*12 ± 4*
	$OxyC_{tei}$	***1-L**-PCP-X_{tei}*	*13 ± 2*

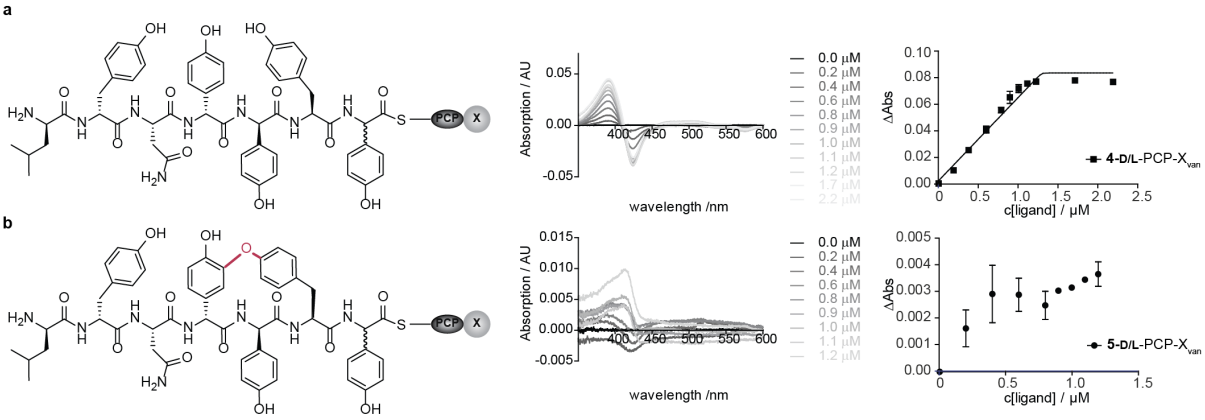

Figure S14. UV-visible spectroscopic binding studies of *peptidyl*-PCP-X_{van} binding to $OxyB_{van}$; Linear peptide (**4-D/L**, **a**), monocyclic peptide (**5-D/L**, **b**).

Table S5. Summary of UV-visible binding studies of $OxyB_{van}$.

4-D/L-PCP-X_{van} binding to $OxyB_{van}$					
Parameter	*Value*	*SE*	*Mean*	*Min*	*Max*
K_D (4-D/L-PCP-X_{van}) [µM]	*< 1*[a]	*n.d.*	*n.d.*	*n.d.*	*n.d.*
ΔA_{max} (4-D/L-PCP-X_{van})	*0.064*	*1.6E-03*	*n.d.*	*n.d.*	*n.d.*
5-D/L -PCP-X_{van} binding to $OxyB_{van}$					
Parameter	*Value*	*SE*	*Mean*	*Min*	*Max*
K_D (5-D/L-PCP-X_{van}) [µM]	*n.d.*[b]	*n.d.*	*n.d.*	*n.d.*	*n.d.*
ΔA_{max} (5-D/L-PCP-X_{van})	*n.d.*	*n.d.*	*n.d.*	*n.d.*	*n.d.*

[a] active site titration. [b] Binding did not evoke Type-I spectral shifts and could thus not be fitted.

References

1) Dordine, R. L., Paneth, P., and Anderson, V. E. (1995) 13C NMR and 1H-1H NOEs of Coenzyme-A: Conformation of the Pantoic Acid Moiety. *Bioorg. Chem. 23*, 169–181.

(2) Haslinger, K., Peschke, M., Brieke, C., Maximowitsch, E., and Cryle, M. J. (2015) X-domain of peptide synthetases recruits oxygenases crucial for glycopeptide biosynthesis. *Nature*.

(3) Brieke, C., Peschke, M., Haslinger, K., and Cryle, M. J. (2015) Sequential In Vitro Cyclization by Cytochrome P450 Enzymes of Glycopeptide Antibiotic Precursors Bearing the X-Domain from Nonribosomal Peptide Biosynthesis. *Angew. Chemie - Int. Ed. 54*, 15715–15719.

(4) Bogomolovas, J., Simon, B., Sattler, M., and Stier, G. (2009) Screening of fusion partners for high yield expression and purification of bioactive viscotoxins. *Protein Expr. Purif. 64*, 16–23.

(5) Haslinger, K., Maximowitsch, E., Brieke, C., Koch, A., and Cryle, M. J. (2014) Cytochrome P450 OxyBtei Catalyzes the First Phenolic Coupling Step in Teicoplanin Biosynthesis. *ChemBioChem 15*, 2719–2728.

(6) Sunbul, M., Marshall, N. J., Zou, Y., Zhang, K., and Yin, J. (2009) Catalytic Turnover-Based Phage Selection for Engineering the Substrate Specificity of Sfp Phosphopantetheinyl Transferase. *J. Mol. Biol. 387*, 883–898.

(7) Ehresmann, B., Imbault, P., and Well, J. H. (1973) Spectrophotometric determination of protein concentration in cell extracts containing tRNA's and rRNA's. *Anal. Biochem. 54*, 454–463.

(8) Kuzmic, P. (1996) Program DYNAFIT for the analysis of enzyme kinetic data: application to HIV proteinase. *Anal. Biochem. 237*, 260–73.

(9) Woithe, K., Geib, N., Zerbe, K., Dong, B. L., Heck, M., Fournier-Rousset, S., Meyer, O., Vitali, F., Matoba, N., Abou-Hadeed, K., and Robinson, J. a. (2007) Oxidative phenol coupling reactions catalyzed by OxyB: A cytochrome P450 from the vancomycin producing organism. Implications for vancomycin biosynthesis. *J. Am. Chem. Soc. 129*, 6887–6895.

(10) Gronenborn, A., Filpula, D., Essig, N., Achari, A., Whitlow, M., Wingfield, P., and Clore, G. (1991) A novel, highly stable fold of the immunoglobulin binding domain of streptococcal protein G. *Science 253*, 657–661.